Evaluation of Patients with Paramyotonia at ^{23}Na MR Imaging during Cold-induced Weakness[1]

Marc-André Weber, MD, MSc
Sonia Nielles-Vallespin, PhD, MSc
Hagen B. Huttner, MD
Johannes C. Wöhrle, MD
Karin Jurkat-Rott, MD, PhD
Frank Lehmann-Horn, MD, PhD
Lothar R. Schad, PhD
Hans-Ulrich Kauczor, MD
Marco Essig, MD
Hans-Michael Meinck, MD

Purpose: To prospectively examine whether sodium 23 (^{23}Na) magnetic resonance (MR) imaging can be used to visualize acute intracellular Na^+ accumulation and the effects of specific therapy in patients with paramyotonia congenita (PC).

Materials and Methods: Ethics committee approval and informed consent were obtained. Sixteen patients (four women, 12 men; mean age, 46.7 years ± 16.7 [standard deviation]) with confirmed PC and 10 healthy volunteers (three women, seven men; mean age, 26.6 years ± 3) were examined by using a 1.5-T MR system with a 16.8-MHz surface coil. ^{23}Na MR imaging was performed before and after local cooling of the nondominant lower leg and exercising, with experimentally induced weakness scored by a neurologist. The ^{23}Na MR examination was repeated in 13 patients and all volunteers after 3 days and, additionally, in seven patients after 4 days of oral administration of mexiletine, which blocks Na^+ channels. The ^{23}Na MR protocol comprised two-dimensional (2D) fast low-angle shot (FLASH), 2D radial, and free induction decay (FID) sequences. The FID data were fitted to a biexponential decay curve to evaluate the slow and fast components of the T2 relaxation time. Fast and slow components were assigned to intra- and extracellular Na^+ concentrations, respectively. Radial and FLASH MR images were evaluated by means of a region-of-interest analysis by using 0.3% saline solution for reference. T1- and T2-weighted MR imaging were also performed. Data were analyzed by using a parametric *t* test.

Results: After exercising, all patients developed considerable weakness exclusively in the cooled lower leg; no weakness was observed in volunteers. In patients, all ^{23}Na MR images showed a significant increase in ^{23}Na signal intensity in the cooled lower leg ($P < .001$) in comparison with nonsignificant findings in volunteers. After treatment with mexiletine, cooling and exercise induced almost no muscle weakness and no changes in ^{23}Na MR signal intensity in patients.

Conclusion: ^{23}Na MR imaging enables visualization of muscular Na^+ accumulation associated with muscle weakness in patients with PC, and effects of specific therapy can be detected.

[1] From the Department of Radiology (M.A.W., H.U.K., M.E.) and Department of Medical Physics in Radiology (S.N., L.R.S.), German Cancer Research Center, Im Neuenheimer Feld 280, D-69120 Heidelberg, Germany; Department of Neurology, University of Heidelberg, Heidelberg, Germany (H.B.H., H.M.M.); Department of Neurology, University Hospital Mannheim, University of Heidelberg, Mannheim, Germany (J.C.W.); and Department of Applied Physiology, University of Ulm, Ulm, Germany (K.J., F.L.). From the 2004 RSNA Annual Meeting. Received May 1, 2005; revision requested June 30; revision received July 24; final version accepted August 25. Supported by the Medical School Research Council of the University of Heidelberg (196/2002) and by the German Research Foundation (DFG, JU470/1). **Address correspondence to** M.A.W. (e-mail: *m.a.weber@dkfz.de*).

Paramyotonia congenita (PC) is an inherited muscular Na^+ channelopathy. In PC, exposure to cold in combination with muscle exercise leads to muscle stiffness and myotonia followed by muscle weakness due to intracellular Na^+ accumulation. These symptoms will disappear spontaneously within a few hours if the patient is no longer exposed to the stimulus (1). PC is caused by autosomal-dominant point mutations, such as T1313M and R1448C, in the voltage-gated muscle membrane Na^+ channel encoded by the *SCN4A* gene (1). Muscle stiffness and weakness are caused by a long-lasting depolarization of muscle fiber membranes. The underlying pathogenetic mechanism is a gating defect of the Na^+ channel, thereby destabilizing the inactivated state—that is, the channel inactivation may be slow or incomplete, causing a long-lasting depolarizing Na^+ inward current (1). The resulting elevated intracellular Na^+ levels lead to membrane depolarization and weakness (1). Muscle stiffness and weakness can be effectively prevented by local anesthetics and class IB antiarrhythmics (1). The agent of choice is mexiletine, which selectively blocks the pathologically inactivating Na^+ channels (2). Treatment is necessary only in a minority of patients to prevent cold- and exercise-induced myotonia and weakness in cold surroundings. Because the elevated myoplasmic Na^+ level can be controlled in vivo—that is, triggered by cooling and exercise and blocked by mexiletine—PC is the ideal disorder for which to establish a clinically feasible sodium 23 (^{23}Na) magnetic resonance (MR) imaging protocol.

Advances in Knowledge

- ^{23}Na MR imaging can depict pathologic myoplasmic Na^+ accumulation associated with muscle weakness in the muscular Na^+ channelopathy paramyotonia congenita.
- ^{23}Na MR imaging can depict the beneficial effect of an Na^+ channel blocking agent.
- A striking intracellular Na^+ accumulation can be observed in muscles in those patients who had normal findings or only mild degeneration at ^{1}H MR imaging.

^{23}Na MR imaging is an MR technique that allows for noninvasive measurement of the Na^+ concentration within tissues. Elevated signal intensity on ^{23}Na MR images has been shown to correspond to high tissue Na^+ concentration due to intracellular Na^+ accumulation and loss of myocardial viability (3). The method is able to discriminate between viable and nonviable myocardial tissue (4,5). The ^{23}Na signal in vivo decays biexponentially, with a fast (0.5–3.0 msec) and a slow (15–30 msec) component. To measure the total ^{23}Na signal, sequences with short echo times are necessary. Authors of previous studies have used ^{23}Na MR imaging to quantify the Na^+ content in skeletal muscles of patients with progressive hereditary degenerative diseases, such as myotonic dystrophy (6,7). However, in vivo data on skeletal muscle Na^+ concentration in muscular channelopathies are lacking. Na^+ channelopathies are especially interesting because they could serve as a paradigm to evaluate different ^{23}Na MR imaging techniques. As a clinical model, we chose PC because its Na^+ channels conduct a higher amount of Na^+ than do physiologic channels, and this results in a myoplasmic Na^+ accumulation associated with muscle stiffness and weakness.

Thus, the aim of our study was to prospectively examine whether ^{23}Na MR imaging can be used to visualize acute intracellular Na^+ accumulation and the effects of specific therapy in patients with PC.

Materials and Methods

Patients and Volunteers

Sixteen patients (four women, 12 men; mean age, 46.7 years ± 16.7 [standard deviation]) with clinically proved PC were included in the study from November 2003 to January 2005. All patients had typical symptoms of PC, with stiffening and weakness of muscles after exercise and exposure to cold. No patient had any sensory impairment at the time of examination. To confirm mutations typical of PC, whole blood (20 mL from each patient) anticoagulated in ethylenediaminetetraacetic acid was taken for *SCN4* mutation analysis. Prior to patient enrollment, from July 2003 to November 2003, 10 healthy volunteers (three women, seven men; mean age, 26.6 years ± 3) with no evidence or history of muscular or cardiovascular disease and no family history of PC (all with normal muscle strength and normal hydrogen 1 [^{1}H] MR imaging findings) were examined for comparison. The study was approved by the ethics committee of Heidelberg University and Ulm University and was conducted according to the Declaration of Helsinki. Informed consent was obtained from all volunteers and patients after the nature of the examination had been fully explained.

Detection of PC Mutation

Mutation screening was performed by two physiologists (K.J. and F.L., with 10 and 20 years of experience, respectively) by using polymerase chain reaction amplification of *SCN4A* exons 22 and 24 as described previously (8). Polymerase chain reaction products were loaded on 2% agarose gel and stained with ethidium bromide, and the band was cut out under ultraviolet light. Bands were purified and cycle-sequenced with 1 pmol of primer by using

Published online before print
10.1148/radiol.2401050737

Radiology 2006; 240:489–500

Abbreviations:
FID = free induction decay
FLASH = fast low-angle shot
PC = paramyotonia congenita
2D = two-dimensional

Author contributions:
Guarantor of integrity of entire study, M.A.W.; study concepts/study design or data acquisition or data analysis/interpretation, all authors; manuscript drafting or manuscript revision for important intellectual content, all authors; manuscript final version approval, all authors; literature research, M.A.W., S.N., F.L., H.M.M.; clinical studies, M.A.W., S.N., H.B.H., J.C.W., K.J., F.L., H.M.M.; statistical analysis, M.A.W., S.N., F.L.; and manuscript editing, M.A.W., S.N., J.C.W., K.J., F.L., L.R.S., H.M.M.

Authors stated no financial relationship to disclose.

the dye terminator kit (Applied Biosystems, Foster City, Calif). Sequencing was performed on 6% denaturating polyacrylamide gels in an ABI 377 HT automated sequencer (Applied Biosystems). All sequences with base exchanges were verified by reverse sequencing of a new polymerase chain reaction product of the same DNA sample. A radiologist (M.A.W.) compared the muscular Na^+ accumulation after cooling and exercise detected at ^{23}Na MR imaging with the detected mutations to elucidate possible relationships between Na^+ channel mutation and Na^+ influx.

Examination Protocol

In patients and volunteers, ^{23}Na MR imaging was performed before and after provocation (ie, local cooling of the nondominant left lower leg and exercising). The contralateral lower leg was not cooled and served as the reference leg. Cooling was performed for 10 minutes with ice pads wrapped around the nondominant lower leg while the subject rested on a stretcher. Then, immediately after cooling, subjects had to bend their knees 30 times and stand on their tiptoes 30 times. This standardized exercise procedure induced local muscle weakness of the cooled lower leg in all patients. The exercise procedure was discontinued as soon as the patient was unable to perform the exercise because of severe paresis; this was done in order to avoid a paralysis that might have lasted for several hours. Fourteen of 16 patients and all volunteers were able to perform the whole exercise procedure. Two of the 16 examined patients received mexiletine (Mexitil; Boehringer Ingelheim, Ingelheim, Germany) as permanent therapy, so no MR examination could be performed without Na^+ channel blockage. These two patients were examined only once.

The muscle strength before and immediately after cooling of the nondominant lower leg and the exercise procedure, as well as muscle strength 45 minutes after the experimentally induced paresis (ie, after the second part of the MR examination), was scored on a six-point scale according to the grading system proposed by the British Medical Research Council (9): score of 0, complete paralysis; 1, minimal contraction; 2, active movement with gravity eliminated; 3, weak contraction against gravity; 4, active movement against gravity and resistance; and 5, normal strength. Examination of the lower limb comprised strength testing of the following: hip flexion, hip extension, hip abduction, hip adduction, knee flexion, knee extension, dorsiflexion, plantar flexion, and eversion of the foot, toe dorsiflexion, and toe plantarflexion. Muscle strength analysis was performed by two neurologists (J.C.W. and H.M.M., with 15 and 30 years of experience in muscular diseases, respectively). The whole experiment, including MR imaging, cooling and exercise, and muscle strength testing, was repeated in 13 patients and in all volunteers after a mean of 3 days. Of the 14 patients who were not undergoing permanent therapy, one was unavailable for repeated testing.

MR Imaging

The study was performed with a 1.5-T clinical MR system (Magnetom Symphony; Siemens Medical Solutions, Er-

Figure 1

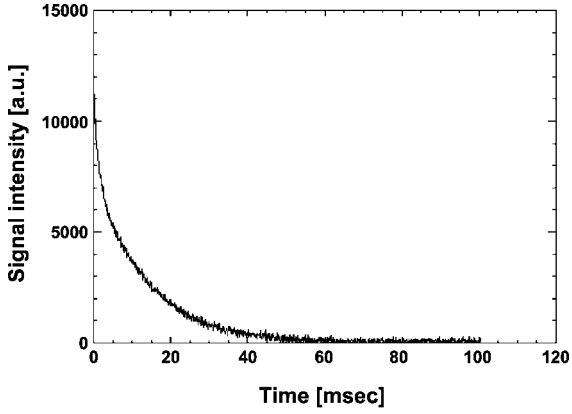

Figure 1: Graph shows ^{23}Na FID data representative for all measured FIDs to evaluate the T2 MR signal decay. The FID data clearly show that the last points are already background noise, thus indicating that acquisition time was long enough to fit the envelope. *a.u.* = arbitrary units.

Table 1

Muscle Strength in Patients with PC before, Immediately after, and 45 Minutes after Provocation

Muscle Group and Test	Cooled Leg			Reference Leg		
	Before	Immediately After	After 45 Minutes	Before	Immediately After	After 45 Minutes
Knee						
Extension	5.0 ± 0.0	4.9 ± 0.4	4.9 ± 0.2	5.0 ± 0.0	5.0 ± 0.0	5.0 ± 0.0
Flexion	5.0 ± 0.1	4.8 ± 0.5	4.9 ± 0.2	5.0 ± 0.0	5.0 ± 0.0	5.0 ± 0.0
Foot						
Dorsiflexion	4.9 ± 0.4	3.8 ± 0.8*	4.2 ± 0.6*	5.0 ± 0.1	4.9 ± 0.2	5.0 ± 0.1
Plantarflexion	4.9 ± 0.2	4.3 ± 0.6*	4.6 ± 0.4*	4.9 ± 0.2	4.9 ± 0.3	4.9 ± 0.3
Eversion	4.9 ± 0.3	4.0 ± 0.5*	4.2 ± 0.4*	4.9 ± 0.3	4.9 ± 0.3	4.9 ± 0.3
Toe						
Dorsiflexion	4.9 ± 0.4	3.7 ± 0.6*	4.1 ± 0.6*	4.9 ± 0.3	4.9 ± 0.3	4.9 ± 0.3
Plantarflexion	4.8 ± 0.4	4.1 ± 0.6*	4.4 ± 0.4*	4.9 ± 0.4	4.9 ± 0.4	4.9 ± 0.4

Note.—Data are mean ± standard deviation. Provocation included cooling of the nondominant lower leg and exercise of both legs. Muscle strength was scored according to the grading system proposed by the British Medical Research Council.

* Statistically significant difference ($P < .05$) between values before and after provocation.

langen, Germany) that was equipped with hardware for broadband spectroscopy by using a 32 × 39-cm single-resonant (16.84-MHz) ^{23}Na surface-quadrature coil (Rapid Biomed, Wuerzburg, Germany) placed over the triceps surae muscles for ^{23}Na measurements and a whole-body coil for ^{1}H measurements. ^{23}Na MR imaging was performed before and after local cooling of the nondominant lower leg and exercising.

^{23}Na MR Imaging Protocol

The ^{23}Na signal in vivo decays biexponentially, with a fast (0.5–3.0 msec) and slow (15–30 msec) component of the T2 relaxation time. The fast component has been previously related to the intracellular Na^+ concentration and the slow component to the extracellular Na^+ concentration (10). In order to measure the total Na^+ signal, it was proposed that sequences with short echo times of less than a millisecond are needed (7). In this case, a weighted average of intracellular and extracellular Na^+ concentration was observed. However, as long as the tissue is adequately perfused, the extracellular Na^+ concentration will remain constant, so changes in ^{23}Na MR signal intensity will directly relate to changes in the intracellular concentration of Na^+ (11). Therefore, a two-dimensional (2D) radial gradient-echo ^{23}Na MR sequence was implemented, which images k-space in a starlike fashion immediately after section selection; the readout gradient and the signal acquisition start simultaneously, achieving an echo time of 0.6 msec. An off-line reconstruction was implemented to regrid the radially acquired data with nearest-neighbor interpolation (taking ramp sampling into account) onto a cartesian grid, followed by a conventional 2D fast Fourier transform by using the IDL software package (version 5.3; Research Systems IDL, Boulder, Colo) (12).

To observe the influence of different echo times on the measured muscular ^{23}Na MR signal intensity, we used three different ^{23}Na MR sequences, with echo times ranging from 0.2 to 3.53 msec. The ^{23}Na MR imaging protocol comprised the ^{23}Na 2D radial gradient-echo sequence (repetition time msec/echo time msec, 13/0.6; resolution, 3.9 × 3.9 × 30 mm; bandwidth, 190 Hz/pixel; number of acquisitions, 400; acquisition

Figure 2

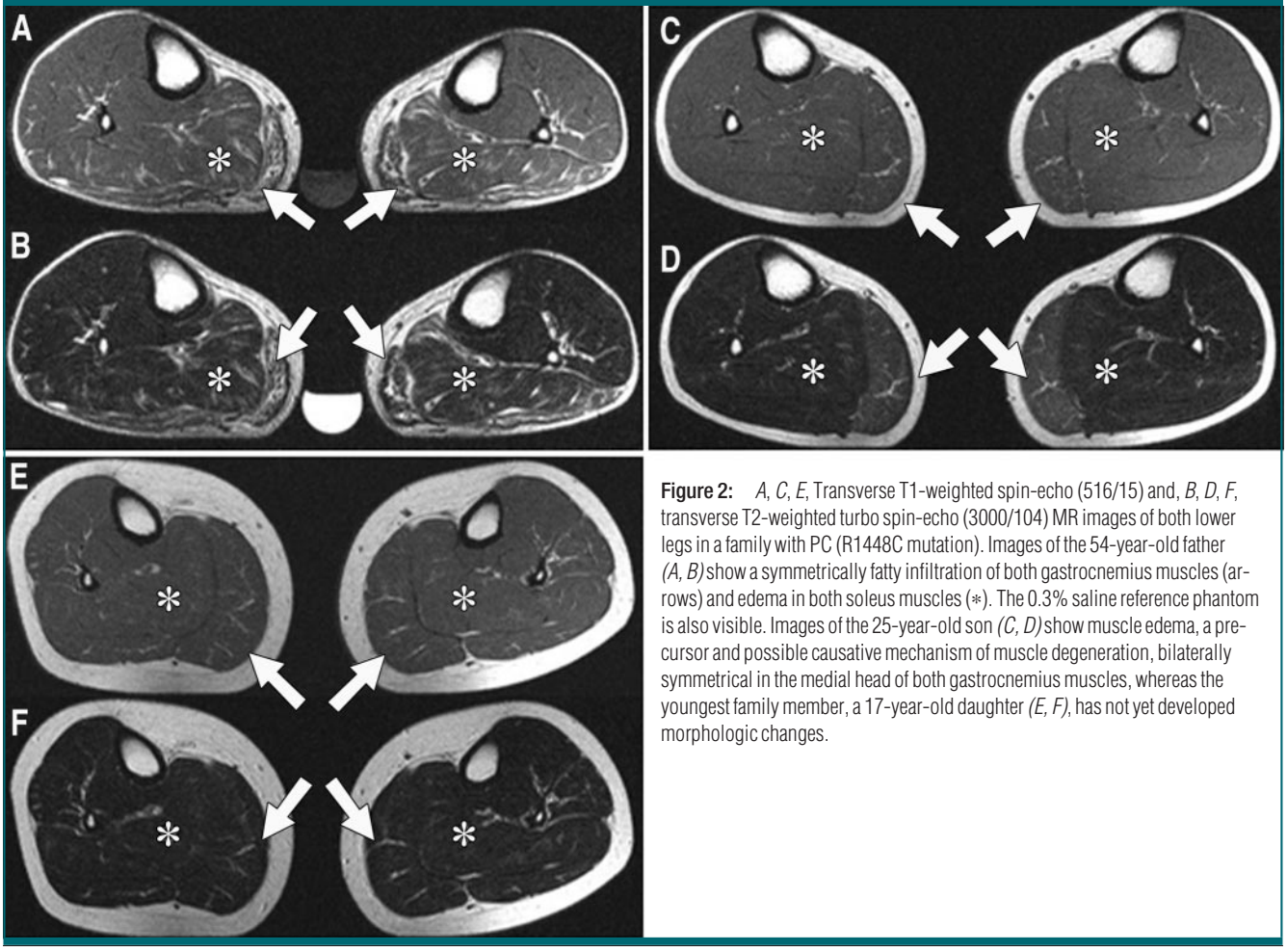

Figure 2: *A, C, E,* Transverse T1-weighted spin-echo (516/15) and, *B, D, F,* transverse T2-weighted turbo spin-echo (3000/104) MR images of both lower legs in a family with PC (R1448C mutation). Images of the 54-year-old father *(A, B)* show a symmetrically fatty infiltration of both gastrocnemius muscles (arrows) and edema in both soleus muscles (*). The 0.3% saline reference phantom is also visible. Images of the 25-year-old son *(C, D)* show muscle edema, a precursor and possible causative mechanism of muscle degeneration, bilaterally symmetrical in the medial head of both gastrocnemius muscles, whereas the youngest family member, a 17-year-old daughter *(E, F)*, has not yet developed morphologic changes.

Figure 3

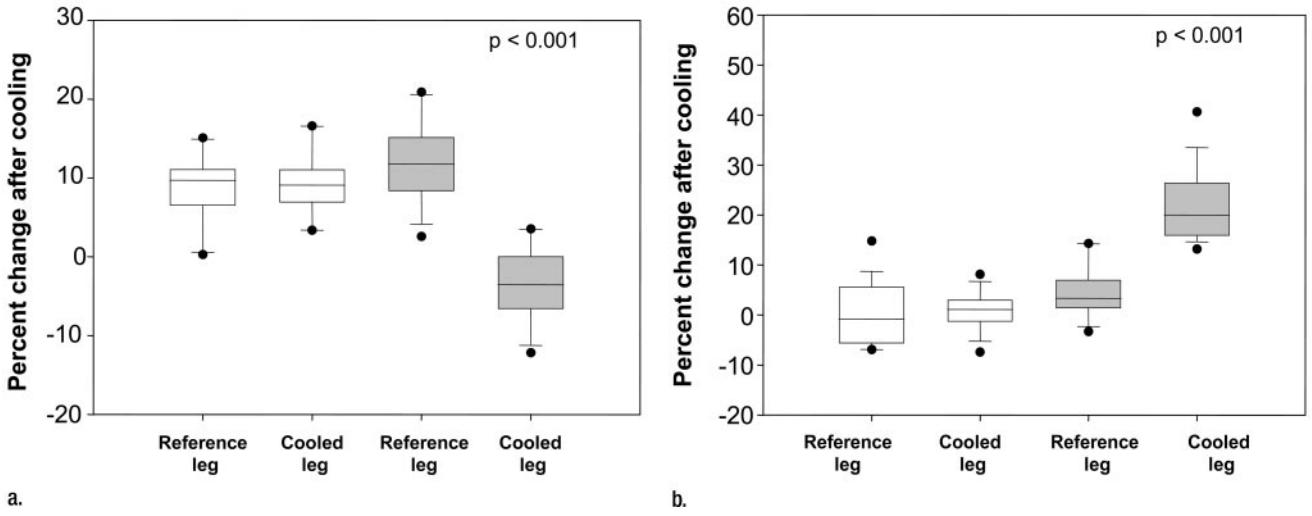

Figure 3: Box plots of percentage change of muscular ^{23}Na MR signal intensity after cooling in patients (gray boxes) and volunteers (white boxes) measured at **(a)** FID and **(b)** 2D radial MR imaging. Boxes show the 25–75 percentile, with a middle line that indicates median; error bars = 10 and 90 percentile; ● = extreme values. FID data (**a**) show a decrease in the ratio of extra-to-intracellular Na^+ concentration after cooling in patients with PC, which reflects intracellular Na^+ accumulation. No change is seen in volunteers or in the reference leg in patients. Two-dimensional radial data (**b**) show Na^+ accumulation in patients with PC by means of an increase in ^{23}Na MR signal intensity in the cooled leg. No change is seen in volunteers.

time, 5.5 minutes) and a ^{23}Na 2D fast low-angle shot (FLASH) sequence (13/3.53; resolution, 2.7 × 2.7 × 30 mm; bandwidth, 190 Hz/pixel; number of acquisitions, 300; acquisition time, 8 minutes). In order to evaluate the T2 signal decay, ^{23}Na free induction decays (FIDs) with a time delay between end of the radiofrequency pulse and start of acquisition (echo time) of 0.2 msec were acquired separately for each lower leg. Further sequence parameters were as follows: repetition time, 1000 msec; bandwidth, 10 kHz; number of points, 1024; and acquisition time, 100 msec.

Analysis of ^{23}Na MR Data

^{23}Na MR imaging with 2D radial and 2D FLASH sequences.—In order to quantify the signal intensity enhancement on the ^{23}Na MR images after exercise and local cooling of the nondominant lower leg, 2D radial and 2D FLASH images were evaluated by means of region-of-interest analysis by using a 0.3% saline solution phantom placed between the lower legs as a reference. Regions of interest had a size of 100 pixels and were placed on both 2D FLASH and 2D radial ^{23}Na MR images by a neurologist and radiologist in consensus (M.A.W. and H.B.H., with 5 and 3 years of experience in their specialties, respectively). A region of interest was placed on the soleus muscle of each lower leg by using the ^{1}H MR images for reference, and a third region of interest was placed on the 0.3% saline solution phantom. The signal intensity on 2D radial and 2D FLASH ^{23}Na MR images was normalized to the 0.3% saline solution phantom for interindividual and intraindividual comparisons—that is, the values of the regions of interest placed on the soleus muscles were divided by the values of the phantom. The signal intensities before and after provocation were analyzed separately for each lower leg. Signal intensity (SI) alterations were considered to reflect changes in muscular Na^+ concentration. The percentage change between the normalized muscular ^{23}Na MR imaging signal intensity before (SI_{pre}) and after (SI_{post}) provocation (ΔSI%) was calculated, and findings were expressed according to Equation (1):

$$\Delta SI\% = \frac{SI_{post} - SI_{pre}}{SI_{pre}} \cdot 100. \quad (1)$$

^{23}Na FID.—The acquired FID data (Fig 1) were fitted to the biexponential decay by using a Levenberg-Marquard algorithm to evaluate the fast ($T2_{fast}$) and slow ($T2_{slow}$) component of the T2 relaxation time, as shown in Equation (2):

$$SI = M_{fast}e^{-t/T2_{fast}} + M_{slow}e^{-t/T2_{slow}}. \quad (2)$$

M_{fast} and M_{slow} are the signals from the fast (ie, $T2_{fast}$) and slow (ie, $T2_{slow}$) component, respectively, and have been related to the intra- and extracellular Na^+ concentrations (10); t indicates time. The envelope of the decay that gives an estimate of the T2* of the sample was used for the fit. The difference between a true T2 measurement and an estimate of T2* for these experiments was about 15% for the long component and 1% for the short component. No B_1 corrections were performed. FID data before and after provocation were analyzed separately for each lower leg. Then the ratio $X = M_{slow}/M_{fast}$ before (X_{pre}) and after (X_{post}) provocation was analyzed separately for each lower leg, and the percentage change after provocation (ΔX%) was calculated according to Equation (3):

$$\Delta X\% = \frac{X_{post} - X_{pre}}{X_{pre}} \cdot 100. \quad (3)$$

Assuming that M_{fast} mainly relates to intracellular Na^+ concentration and

M_{slow} mainly relates to extracellular Na^+ concentration, and since extracellular concentration of Na^+ remains constant due to perfusion (11), a decrease in M_{slow}/M_{fast} should reflect an accumulation of intracellular Na^+. The percentages of change measured according to Equations (1) and (3) by using the different ^{23}Na MR sequences were analyzed for a possible correlation.

^{1}H MR imaging.—In order to exclude other muscular pathologic conditions, ^{1}H MR imaging was performed in addition to the ^{23}Na MR imaging protocol before provocation. The ^{1}H MR imaging protocol comprised a transverse T1-weighted spin-echo sequence (516/15, matrix of 308 × 512, section thickness of 6 mm) and a transverse T2-weighted turbo spin-echo sequence (3000/104, matrix of 308 × 512, section thickness of 6 mm). Image interpretation was performed by two readers (M.A.W. and M.E., with 5 and 11 years of experience in musculoskeletal MR imaging, respectively) in consensus. A muscle edema was defined as an area of localized hyperintensity on T2-weighted MR images. Fatty infiltration, which was defined as areas with signal intensity equivalent to that of subcutaneous fat on T1- and T2-weighted MR images, was interpreted as a sign of chronic myopathy. The MR imaging criterion of muscle atrophy was a reduction of muscle cross-sectional area, which was assessed qualitatively by the two readers in consensus by using the opposite side or other muscle groups for comparison. The readers were asked to assess in a dichotomous fashion whether these criteria were identified.

Na^+ Channel Blockage

In seven patients with PC and no history of cardiac disease (one woman, six men; mean age, 39 years ± 14), a third experiment that included ^{23}Na MR imaging, cooling, and muscle strength testing was performed after 4 days of oral medication with a selective Na^+ channel blocker (200 mg of mexiletine [Mexitil; Boehringer Ingelheim] three times a day).

Before medication was administered, informed consent was again obtained from the patients. Because of the fact that, in rare cases, cardiac arrhythmias can be induced by mexiletine, electrocardiography was performed before medication was administered. The electrocardiogram was normal in all of these seven patients, and there were no adverse events related to this third experiment. Among the other six patients available for repeated testing, two reported that they had developed side effects after previous mexiletine administration, two had cardiac arrhythmias, and two did not give informed consent, so no mexiletine could be administered. The Na^+ channel blocker was not given to the volunteers, in order to prevent unnecessarily exposing them to the risk of adverse events.

Statistical Analysis

Data entry procedures and statistical analysis were performed with a statistical analysis software system (SPSS for Windows, version 11.5.1, 2002; SPSS, Chicago, Ill). Data were analyzed by using a two-sided parametric *t* test for testing no difference versus difference

Figure 4

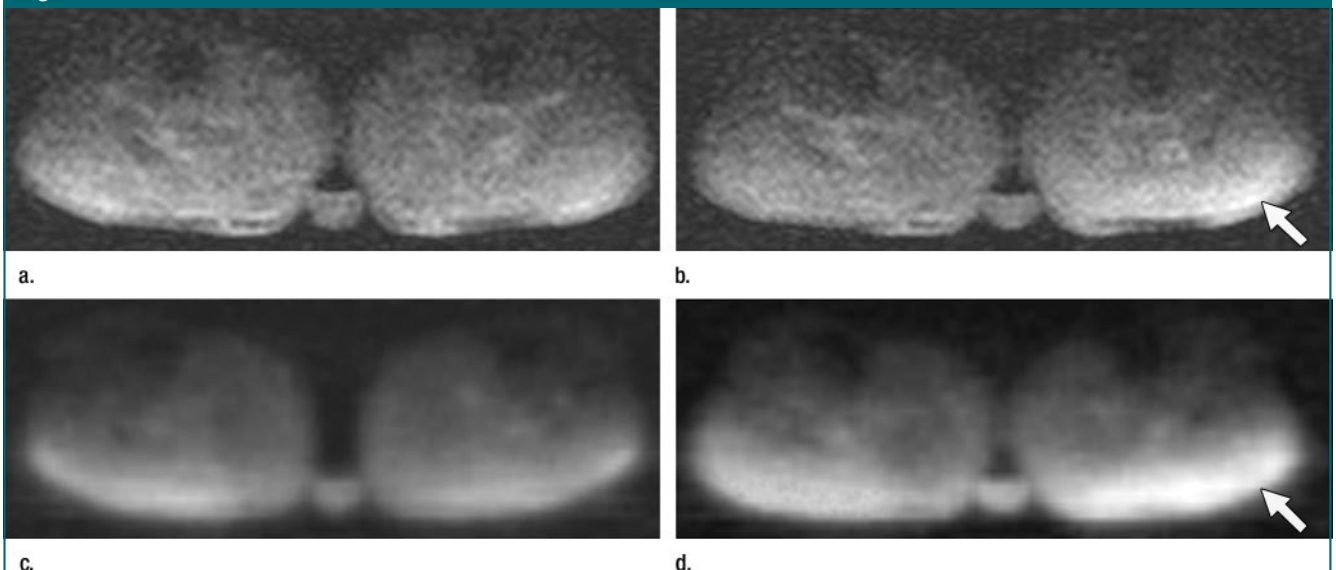

Figure 4: **(a, b)** Transverse 2D FLASH (13/3.53) and **(c, d)** transverse 2D radial (13/0.6) ^{23}Na MR images of both lower legs, before and after provocation, show Na^+ accumulation in a 39-year old patient (T1313M mutation). Images after cooling (**b**, **d**) show signal intensity increase in the cooled left leg (arrow). B_1 field inhomogeneity caused by the surface coil, with a penetration depth of 7.8 cm, leads to highest intensity near the coil windings. The pathologic signal intensity increase can be evaluated because the right (reference) leg is the same distance from the coil and thus submitted to a similar B_1 field. The radial images have blurring due to decay of the short T2 component during data acquisition. The 0.3% saline solution phantom is seen between the lower legs. Blood vessels and bones appear as areas of high and low signal intensity, respectively (7).

and by using one-sided *t* tests for testing no difference against larger or smaller (level of significance, $P = .05$). Results were expressed as mean ± standard deviation. For each difference found in our study, the corresponding statistical power was calculated by using the effect size approach (nQuery Advisor version 5.0, 2002; Statistical Solutions, Saugus, Mass). For each statistically significant difference, the corresponding statistical power was at least 80%.

Results

Mutation Screening

In all 16 patients, a typical PC mutation was identified: amino acid substitution R1448C in eight patients, T1313M in five patients, and R1448H in three patients.

Muscle Strength

In patients with PC, the muscle strength prior to cooling and exercise was normal in both legs, and the muscle strength after exercise was normal in the noncooled leg (Table 1). Hip muscle function was not influenced by cooling of the lower leg and exercise. All 16 patients with PC presented with muscle weakness in the cooled lower leg, particularly for foot and toe dorsiflexion. Muscle strength was partially recovered 45 minutes after cooling and exercise (British Medical Research Council score: before cooling, 4.9 ± 0.1; immediately after cooling, 4.2 ± 0.5; 45 minutes after cooling, 4.5 ± 0.3). In 13 of 13 patients, there was no significant intraindividual variability between the muscle strength scored during the first experiment and the second experiment 3 days later ($P = .07$). In all 10 volunteers, muscle strength was normal for all conditions.

^{1}H MR Imaging Results

In six of 16 patients (three women, three men; mean age, 40 years ± 18; T1313M, R1448C, and R1448H mutations in two patients each), muscles of the lower leg were normal on T1-weighted and T2-weighted MR images. In two male patients with R1448C (ages, 25 and 42 years), a bilaterally symmetric homogeneous edema was observed before exercise that was confined to the medial head of the gastrocnemius muscle (Fig 2). In one female and seven male patients (mean age, 55 years ± 13; mutations: R1448H in one patient, T1313M in three patients, and R1448C in four patients), a bilaterally symmetric increased signal intensity of the medial head of the gastrocnemius muscle on T1- and T2-weighted MR images was detected that was interpreted as a fatty infiltration (Fig 2). There was no muscle atrophy in any of the 16 patients with PC. In all 10 volunteers, results at MR imaging were normal.

Table 2

Percentage Change in Muscular ^{23}Na MR Imaging Signal Intensity after Provocation

MR Imaging Sequence	Patients		Volunteers	
	Cooled Leg (%)	Reference Leg (%)	Cooled Leg (%)	Reference Leg (%)
FID (echo time, 0.2 msec)*	14 ± 5†	−2 ± 5	1 ± 4	1 ± 5
2D radial (echo time, 0.6 msec)‡	22 ± 9†	4 ± 6	1 ± 4	0 ± 7
2D FLASH (echo time, 3.53 msec)‡	8 ± 12†	−2 ± 8	0 ± 3	−1 ± 3

Note.—Data are mean ± standard deviation. Negative values correspond to reduction of muscular ^{23}Na signal intensity after provocation.

* Percentage change measured according to Equation (3).

† Statistically significant difference ($P < .05$) between cooled and reference leg.

‡ Percentage change measured according to Equation (1).

Table 3

Measurement of ^{23}Na MR Imaging Signal Intensity

Group and Parameter	2D FLASH Imaging*	2D Radial Imaging*	FID Imaging†
Volunteers			
Cooled leg			
Before provocation	0.93 ± 0.11	0.89 ± 0.18	2.04 ± 0.28
After provocation	0.93 ± 0.10	0.90 ± 0.18	2.02 ± 0.31
Reference leg			
Before provocation	0.93 ± 0.09	0.92 ± 0.17	2.05 ± 0.36
After provocation	0.92 ± 0.10	0.92 ± 0.17	2.01 ± 0.32
Patients			
Cooled leg			
Before provocation	1.15 ± 0.23	1.02 ± 0.12	1.98 ± 0.34
After provocation	1.23 ± 0.23‡	1.24 ± 0.14‡	1.70 ± 0.27‡
Reference leg			
Before provocation	1.17 ± 0.23	1.03 ± 0.11	1.85 ± 0.36
After provocation	1.14 ± 0.21	1.07 ± 0.15‡	1.89 ± 0.39

Note.—Data are mean ± standard deviation.

* Data are muscular ^{23}Na signal intensity values normalized to the 0.3% saline solution reference phantom.

† Data are signal intensity values measured as the ratio of extracellular-to-intracellular Na^{+} concentration.

‡ Statistically significant difference ($P < .05$) between values before and after provocation.

^{23}Na MR Imaging Results

In 14 of 14 patients, ^{23}Na MR images obtained after provocation showed significantly higher ^{23}Na signal intensity in the cooled leg than in the reference leg and in comparison with both legs in volunteers (Figs 3, 4), with low intraindividual variability at subsequent MR examinations (Tables 2–5).

Two-dimensional Radial MR Data

Prior to provocation, in 14 of 14 patients the muscular ^{23}Na MR signal intensity was not significantly different between the lower legs ($P = .48$, Table 3).

After provocation, a significant increase in muscular ^{23}Na MR signal intensity could be observed in the reference leg ($P = .003$), and a more pronounced increase could be observed in the cooled leg ($P < .001$, Table 2), leading to significantly higher muscular ^{23}Na MR signal intensity in the cooled leg than in the reference leg ($P < .001$, Table 3). Muscular ^{23}Na signal intensity was significantly higher in the 14 patients than in the 10 volunteers (reference leg, $P = .01$; cooled leg, $P = .01$), and the percentage change in muscular ^{23}Na signal intensity after provocation was significantly higher in patients than in volunteers (reference leg, $P = .03$; cooled leg, $P < .001$).

In 13 of 13 patients, both before ($P = .25$) and after ($P = .52$) provocation, the muscular ^{23}Na signal intensity was not significantly different between the first experiment and the second experiment 3 days later in the reference leg and cooled leg ($P = .25$ before and $P = .58$ after provocation, Table 4). No significant differences were found in the percentage change of muscular ^{23}Na signal intensity after provocation between the first and second experiment ($P = .83$ for the reference leg and $P = .52$ for the cooled leg, Table 5). In 10 of 10 volunteers, before ($P = .06$) and after ($P = .06$) provocation, the muscular ^{23}Na signal intensity was not significantly different between the lower legs (Table 3), and no significant increase in ^{23}Na signal intensity could be observed in the reference leg ($P = .86$) or in the cooled leg ($P = .41$, Table 2).

Table 4

Constancy of ^{23}Na MR Imaging Measurements at First and Second Experiment in Patients with PC

Leg and Parameter	2D FLASH Imaging*	2D Radial Imaging*	FID Imaging†
Cooled leg			
First experiment			
Before provocation	1.16 ± 0.22	1.03 ± 0.11	2.07 ± 0.44
After provocation	1.23 ± 0.24‡	1.25 ± 0.17‡	1.76 ± 0.33‡
Second experiment			
Before provocation	1.15 ± 0.26	1.00 ± 0.12	1.90 ± 0.19
After provocation	1.22 ± 0.23‡	1.22 ± 0.12‡	1.66 ± 0.21‡
Reference leg			
First experiment			
Before provocation	1.18 ± 0.22	1.04 ± 0.13	1.92 ± 0.45
After provocation	1.13 ± 0.24	1.08 ± 0.18‡	1.96 ± 0.49
Second experiment			
Before provocation	1.16 ± 0.25	1.01 ± 0.09	1.78 ± 0.24
After provocation	1.14 ± 0.20	1.05 ± 0.10	1.81 ± 0.27

Note.—Data are mean ± standard deviation. The second experiment was performed 3 days after the first experiment.

* Data are muscular ^{23}Na signal intensity values normalized to the 0.3% saline solution reference phantom.

† Data are signal intensity values measured as the ratio of extracellular-to-intracellular Na^+ concentration.

‡ Statistically significant difference ($P < .05$) between values before and after provocation.

Table 5

Constancy of Percentage Change in Muscular ^{23}Na MR Imaging Signal Intensity in Patients with PC after Provocation

MR Imaging Sequence	First Experiment		Second Experiment	
	Cooled Leg (%)	Reference Leg (%)	Cooled Leg (%)	Reference Leg (%)
FID*	15 ± 5†	−2 ± 6	13 ± 5†	−1 ± 4
2D radial‡	21 ± 6†	4 ± 5	23 ± 12†	5 ± 8
2D FLASH‡	6 ± 12†	−4 ± 8	8 ± 13†	−1 ± 8

Note.—Data are mean ± standard deviation. Negative values correspond to reduction of muscular ^{23}Na signal intensity after provocation. The second experiment was performed 3 days after the first experiment.

* Percentage change measured according to Equation (3).

† Statistically significant difference ($P < .05$) between cooled and reference leg.

‡ Percentage change measured according to Equation (1).

Two-dimensional FLASH MR Data

In 14 of 14 patients, the ^{23}Na signal intensity increase in the cooled lower leg after provocation was less pronounced on 2D FLASH MR images in comparison with 2D radial MR images (Table 2). Before provocation, ^{23}Na signal intensity was not significantly different between the two legs ($P = .22$), but after provocation, ^{23}Na signal intensity was significantly higher in the cooled leg than in the reference leg ($P < .001$, Table 3), which showed no increase in muscular ^{23}Na signal intensity (mean, −2% ± 8). The ^{23}Na signal intensity was significantly higher in the 14 patients than in the 10 volunteers (reference leg, $P < .001$; cooled leg, $P < .001$). There was no significant difference in percentage change of muscular ^{23}Na signal intensity after provocation

Figure 5

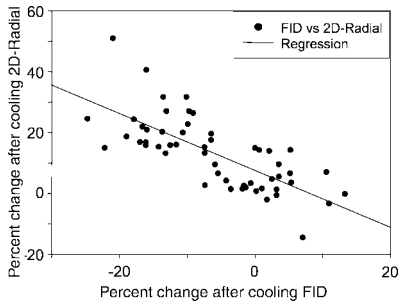

Figure 5: Graph shows correlation of ^{23}Na FID and 2D radial MR data. The percentage change of muscular ^{23}Na signal intensity after cooling in the nondominant lower leg is correlated between FID and 2D radial MR imaging. Linear regression, $r^2 = 0.533$.

Table 6

Muscle Strength before, Immediately after, and 45 Minutes after Provocation in Seven Patients Treated with Na^+ Channel–blocking Agent

Muscle Group and Test	No Na^+ Channel Blockage			Na^+ Channel Blockage		
	Before	Immediately After	After 45 Minutes	Before	Immediately After	After 45 Minutes
Knee						
Extension	5.0 ± 0.0	5.0 ± 0.0	5.0 ± 0.0	5.0 ± 0.0	5.0 ± 0.0	5.0 ± 0.0
Flexion	5.0 ± 0.0	5.0 ± 0.0	5.0 ± 0.0	5.0 ± 0.0	5.0 ± 0.0	5.0 ± 0.0
Foot						
Dorsiflexion	4.9 ± 0.5	3.6 ± 0.8*	3.9 ± 0.6*	5.0 ± 0.0	4.8 ± 0.4	4.9 ± 0.2
Plantarflexion	5.0 ± 0.0	4.4 ± 0.5*	4.7 ± 0.3*	5.0 ± 0.0	5.0 ± 0.0	5.0 ± 0.0
Eversion	4.9 ± 0.3	4.0 ± 0.5*	4.1 ± 0.4*	5.0 ± 0.0	4.7 ± 0.4	4.9 ± 0.2
Toe						
Dorsiflexion	4.9 ± 0.4	3.6 ± 0.7*	3.8 ± 0.7*	5.0 ± 0.0	4.6 ± 0.4*	4.8 ± 0.3
Plantarflexion	4.9 ± 0.2	4.3 ± 0.5*	4.4 ± 0.5*	5.0 ± 0.0	4.9 ± 0.2	5.0 ± 0.0

Note.—Data are mean ± standard deviation for the first two measurements combined (no blockage) versus the third measurement (blockage). Provocation included cooling of the nondominant lower leg and exercise. Muscle strength was scored according to the grading system proposed by the British Medical Research Council.

* Statistically significant difference ($P < .05$) between values before and after provocation.

between the reference leg in the 14 patients and that in the 10 volunteers ($P = .32$), but the percentage change was significantly higher in the cooled leg of patients than in that of volunteers ($P = .003$).

In 13 of 13 patients, both before ($P = .69$) and after ($P = .92$) provocation, the muscular ^{23}Na signal intensity was not significantly different between the first experiment and the second experiment 3 days later in the reference lower leg and the cooled lower leg (Table 4; $P = .68$ before and $P = .91$ after provocation). In 10 of 10 volunteers, the ^{23}Na signal intensity was not significantly different in the lower legs before ($P = .93$) or after ($P = .73$, Table 3) provocation and was not influenced by cooling and exercise (reference leg, $P = .29$; cooled leg, $P = .62$).

FID Data

In 14 of 14 patients with PC, the ratio of extracellular-to-intracellular Na^+ concentration prior to provocation was not significantly different between the two lower legs ($P = .18$). The concentration ratio in the reference leg before and after exercise was also not significantly different ($P = .10$; Table 3). In comparison with the reference leg, there was a significant decrease in extracellular-to-intracellular concentration of Na^+ in the cooled leg after provocation ($P < .001$; Tables 2, 3); this decrease was detected in all patients. There was no difference in percentage change of muscular ^{23}Na signal intensity after provocation between the reference leg in the 14 patients and that in the 10 volunteers ($P = .051$), but there was a significant difference between the cooled leg in the 14 patients and that in the 10 volunteers ($P < .001$; Fig 3a).

In 13 of 13 patients, no significant differences in percentage change of muscular ^{23}Na MR signal intensity after provocation were found between the first experiment and the second experiment 3 days later (reference leg, $P = .94$; cooled leg, $P = .37$; Table 5), and the ratio of extracellular-to-intracellular Na^+ concentration was not significantly different between the first and second experiments in the reference leg before ($P = .09$) and after ($P = .13$; Table 4) provocation and in the cooled leg before ($P = .07$) and after ($P = .07$; Table 4) provocation. In 10 of 10 volunteers, the ratio of extracellular-to-intracellular Na^+ concentration was not significantly different ($P = .89$) in the two legs before provocation and remained unchanged after exercise in the reference leg ($P = .18$) and cooled leg ($P = .57$; Table 3). In 10 of 10 volunteers, no significant increase of percentage change in muscular ^{23}Na signal intensity could be observed after provocation ($P = .72$; Table 2). The correlation between the percentage change in muscular ^{23}Na signal intensity after provocation measured at 2D radial and FID ^{23}Na MR imaging was higher than the other correlations (linear regression, $r^2 = 0.53$; Fig 5), while correlation was low when comparing 2D FLASH with FID (linear regression, $r^2 = 0.12$) and 2D radial (linear regression, $r^2 = 0.13$) MR imaging.

Na^+ Channel Blockage

In seven of seven patients, muscle strength of the cooled lower leg improved after selective Na^+ channel blockage (Table 6), and ^{23}Na MR imaging demonstrated a reduced percentage change in muscular ^{23}Na signal intensity (Table 7, Fig 6) after cooling (2D radial MR imaging, $P = .002$; FID, $P < .001$; and 2D FLASH MR imaging, $P = .10$), whereas no significant changes were observed in the reference leg (2D radial MR imaging, $P = .08$; FID, $P = .31$; and 2D FLASH MR imaging, $P = .83$).

Correlation of Na^+ Accumulation and Mutation

There was no significant difference in Na^+ accumulation between the seven patients with R1448C (three women, four men; mean age, 45 years ± 18) and the five patients with T1313M (one

woman, four men; mean age, 47 years ± 17). The mean percentage change in muscular ^{23}Na signal intensity after provocation in the cooled leg, measured by means of 2D radial MR imaging, was 20% ± 6 for patients with amino acid substitution R1448C and 21% ± 9 for those with T1313M ($P = .75$), and the percentage change in the reference leg was 5% ± 8 for patients with R1448C and 4% ± 5 for those with T1313M ($P = .82$). Both before and after provocation, the muscular ^{23}Na MR imaging signal intensity was not significantly different between patients with T1313M and those with R1448C (Table 8; before provocation: reference leg, $P = .16$; cooled leg, $P = .70$; after provocation: reference leg, $P = .21$; cooled leg, $P = .81$).

Discussion

In our study, all ^{23}Na MR sequences were able to depict pathologic Na^+ accumulation associated with muscle weakness in these patients. The intraindividual variability of our ^{23}Na MR imaging measurements was low. In accordance with previous observations (13), we found no significant changes in muscular ^{23}Na signal intensity in healthy volunteers after exercise.

The observed tissue Na^+ concentration is composed of the weighted average of extracellular and intracellular Na^+ concentrations in the examined tissue. Extracellular Na^+ concentration at 140 mmol/L is about 10-fold higher than intracellular concentration, which is about 10–15 mmol/L (11). Arguably, the more physiologically relevant information is intracellular Na^+ concentration, which reflects the function of Na^+ channels to conduct Na^+ along the electrochemical gradient at the membrane and the cell's ability to pump out Na^+. Extracellular concentration of Na^+ will remain virtually constant as long as there is adequate perfusion of tissue, so that under these circumstances, despite the inability to resolve intra- and extracellular components of the ^{23}Na signal, the use of short echo times, such as 0.6 msec, provides a measurement of intracellular Na^+ concentration (11). The FID sequence with an ultrashort time delay between the end of the radiofrequency pulse and the start of data acquisition showed a muscular Na^+ accumulation after cooling in PC that takes place in the intracellular compartment because of an Na^+ influx from the extracellular compartment; this is because the ratio of extracellular-to-intracellular Na^+ measured by means of FID decreased in the cooled lower leg that developed muscle weakness. The increase in intracellular Na^+ concentration strengthens the hypothesis (10) that the fast component of the T2 relaxation time is associated with intracellular and the

Table 7

Percentage Change in Muscular ^{23}Na MR Imaging Signal Intensity after Provocation in Seven Patients Treated with Na^+ Channel–blocking Agent

MR Imaging Sequence and Leg	No Na^+ Channel Blockage	Na^+ Channel Blockage
FID*		
Reference leg	−0.7 ± 4.5	−2.8 ± 3.7
Cooled leg	14.7 ± 4.4†	0.1 ± 4.3
2D radial‡		
Reference leg	4.5 ± 4.9	−0.6 ± 7.9
Cooled leg	23.3 ± 11.5†	5.4 ± 7.8
2D FLASH‡		
Reference leg	−2.8 ± 9.7	−2.0 ± 4.9
Cooled leg	11.3 ± 14.6†	1.5 ± 4.4

Note.—Data are mean ± standard deviation for the first two measurements combined (no blockage) versus the third measurement (blockage). Negative values correspond to reduction of muscular ^{23}Na signal intensity after provocation.

* Percentage change measured according to Equation (3).

† Statistically significant difference ($P < .05$) between examination with and examination without Na^+ channel blockage.

‡ Percentage change measured according to Equation (1).

Figure 6

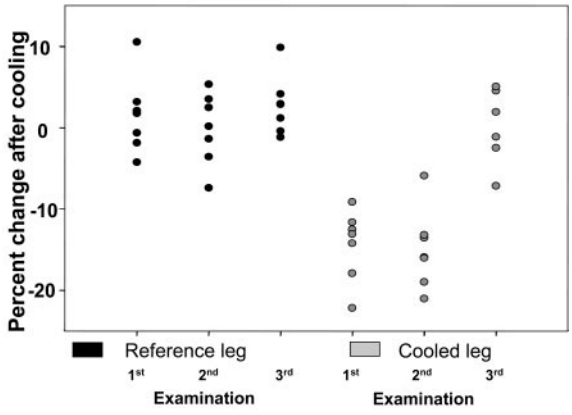

Figure 6: Graph shows results in seven patients with PC before (first and second examination) and after (third examination) blockage of pathologic Na^+ channels. Percentage change of muscular ^{23}Na signal intensity after cooling (measured by means of FID) is shown for each patient. There is a decrease in the extracellular-to-intracellular Na^+ concentration ratio in the cooled leg at the first and second examination (without mexiletine). At the third examination, concomitant with an improvement in muscle strength, there is an increase in the concentration ratio to values comparable to those in the reference leg.

slow component with extracellular Na^+ concentration.

A primary concern when using single-quantum ^{23}Na MR imaging methods is the need to limit signal loss from fast T2 decay by keeping the echo time as short as possible. By using FID, we were able to use a time delay as short as 0.2 msec between the end of the radiofrequency pulse and the start of acquisition. The FID measurements, however, were nonselective, so that ^{23}Na signal from the whole lower leg was acquired. The use of the surface coil minimized this problem because of its small region of sensitivity. For direct visualization of the muscular ^{23}Na signal intensity, we established a 2D radial MR sequence that enables the use of region-of-interest analysis. We demonstrated in our study that although the echo time of the 2D radial sequence is 0.4-msec longer than that of the FID sequence, the results were comparable. Hence, for further analysis of muscular Na^+ content, we recommend the use of radial MR imaging techniques. A limitation of ^{23}Na MR imaging is the low signal-to-noise ratio at 1.5 T and, consequently, the relatively long measurement time. However, our MR imaging protocol was well tolerated by all patients. ^{23}Na MR imaging in muscle is more challenging than that in the brain, because the total Na^+ concentration in muscle is about 32% lower than that in the brain, with 43–45 mmol per kilogram wet weight (7). This translates directly into a reduced signal-to-noise ratio that leads to decreased spatial resolution and prolonged image acquisition times.

One of the advantages of the 2D radial MR technique is that Na^+ accumulation was visualized not only in the cooled muscles of patients but also in the noncooled muscles, which was partially provoked by exercise. In a warm environment, most patients with paramyotonia do not present with myotonic stiffness during rest but become stiff with continued strong activity. This phenomenon is called paradoxical myotonia because it is contrary to the relief of stiffness during repeated contractions in patients with myotonia congenita, a chloride channel disease (warm-up phenomenon). The paradoxical myotonia is caused by reopening of Na^+ channels, which can generate bursts of action potentials leading to muscle stiffness. The current conducted through the reopening Na^+ channels may be responsible for the Na^+ accumulation, which was visualized with the 2D radial MR technique.

Table 8

Correlation of ^{23}Na MR Imaging Signal Intensity and Mutation

PC Mutation	Before Provocation		After Provocation	
	Cooled Leg	Reference Leg	Cooled Leg	Reference Leg
R1448C	1.04 ± 0.14	1.07 ± 0.14	1.26 ± 0.19*	1.13 ± 0.19
T1313M	1.02 ± 0.07	1.01 ± 0.04	1.24 ± 0.10*	1.05 ± 0.05

Note.—Data are mean ± standard deviation. Muscular ^{23}Na signal intensity analyzed with the 2D radial sequence was normalized to the 0.3% saline solution reference phantom.

* Statistically significant difference ($P < .05$) between cooled leg and reference leg.

Moreover, effects of a specific blockage of the pathologic PC Na^+ channels were examined. Muscle stiffness and weakness are prevented by Na^+ channel blockers such as mexiletine (2). Our preliminary data showed that effects of a specific blockage of the pathologically altered Na^+ channels could be monitored in vivo in patients with PC. After a 4-day period of medication with mexiletine, the provocative test caused much smaller Na^+ accumulation and less weakness; thus, the beneficial effect of a drug that exerts its effects at the molecular defect of the disease could be visualized.

To date, reports on ^{23}Na MR imaging have been restricted mainly to pathologic conditions in the heart, such as ischemia (4–5), and those in the brain, such as stroke (14) and tumors (11,15,16), or have focused on imaging of larger organ systems (17,18). To our knowledge, only two studies have dealt with ^{23}Na MR imaging in patients with a muscle disease, myotonic dystrophy. In two (7) and seven (6) patients, the observed myoplasmic Na^+ accumulation correlated with muscle degeneration. Compared with the results of these studies, which suggest that an increased Na^+ concentration in the muscle reflects a sign of irreversible cell necrosis, our results show that even a striking intracellular Na^+ accumulation can be observed in muscles of patients with channelopathies, such as PC, that were normal or only mildly degenerated on ^{1}H MR images.

Limitations of our study were that findings at ^{23}Na MR imaging were correlated with subjective assessment of muscle strength by nonblinded observers by using the British Medical Research Council score. Furthermore, absolute Na^+ concentrations within the muscle tissue were not calculated. We considered the signal-to-noise ratio provided by the measurements at 1.5-T MR as too low, together with the B_1 field inhomogeneity caused by the surface coil, for applying the necessary corrections on the measured data to calculate valid tissue Na^+ concentrations.

The results of our study show that ^{23}Na MR imaging can enable visualization of pathologic Na^+ accumulation in muscle cells that is associated with muscle weakness in patients with the inherited Na^+ channel disease PC. Furthermore, effects of a specific Na^+ channel blockage can be visualized. In our institution, ^{23}Na MR imaging sequences have been introduced to integrate ^{23}Na MR imaging into clinical work-up, thus indicating its potential to evolve from a research topic to a clinically feasible diagnostic tool.

Acknowledgments: The authors thank Ivan Zuna, PhD, for the statistical analysis and Renate Jerecic, PhD, and Heinz-Peter Schlemmer, MD, for their help with the preliminary experiments and the study concept. The support of Achim Bankamp, PhD, with the development of the 2D radial MR data reconstruction is gratefully acknowledged.

References

1. Lehmann-Horn F, Jurkat-Rott K. Voltage-gated ion channels and hereditary disease. Physiol Rev 1999;79:1317–1371.
2. Mohammadi B, Jurkat-Rott K, Alekov AK, Dengler R, Bufler J, Lehmann-Horn F. Preferred mexiletine block of human sodium channels with IVS4 mutations and its pH-dependence. Pharmacogenet Genomics 2005; 15:235–244.
3. Kim RJ, Judd RM, Chen EL, Fieno DS, Parrish TB, Lima JA. Relationship of elevated 23Na magnetic resonance image intensity to infarct size after acute reperfused myocardial infarction. Circulation 1999;100:185–192.
4. Sandstede JJ, Pabst T, Beer M, et al. Assessment of myocardial infarction in humans with (23)Na MR imaging: comparison with cine MR imaging and delayed contrast enhancement. Radiology 2001;221:222–228.
5. Horn M. 23Na magnetic resonance imaging for the determination of myocardial viability: the status and the challenges. Curr Vasc Pharmacol 2004;2:329–333.
6. Kushnir T, Knubovets T, Itzchak Y, et al. In vivo 23Na NMR studies of myotonic dystrophy. Magn Reson Med 1997;37:192–196.
7. Constantinides CD, Gillen JS, Boada FE, Pomper MG, Bottomley PA. Human skeletal muscle: sodium MR imaging and quantification—potential applications in exercise and disease. Radiology 2000;216:559–568.
8. Heine R, Pika U, Lehmann-Horn F. A novel SCN4A mutation causing myotonia aggravated by cold and potassium. Hum Mol Genet 1993;2:1349–1353.
9. Victor M, Ropper AH. Adams and Victor's principles of neurology. 7th ed. New York, NY: McGraw-Hill, 2001; 1464–1479.
10. Narayana PA, Kulkarni MV, Mehta SD. NMR of 23Na in biological systems. In: Partain CL, Price RR, Patton JA, Kulkarni MV, Everette JA Jr, eds. Magnetic resonance imaging. 2nd ed. Vol 2, physical principles and instrumentation. Philadelphia, Pa: Saunders, 1998; 1553–1563.
11. Ouwerkerk R, Bleich KB, Gillen JS, Pomper MG, Bottomley PA. Tissue sodium concentration in human brain tumors as measured with 23Na MR imaging. Radiology 2003;227: 529–537.
12. Jackson J, Meyer C, Nishimura D, Macovski A. Selection of a convolution function for Fourier inversion using gridding. IEEE Trans Med Imaging 1991;10:473–478.
13. Bansal N, Szczepaniak L, Ternullo D, Fleckenstein JL, Malloy CR. Effect of exercise on 23Na MRI and relaxation characteristics of the human calf muscle. J Magn Reson Imaging 2000;11:532–538.
14. Thulborn KR, Gindin TS, Davis D, Erb P. Comprehensive MR imaging protocol for stroke management: tissue sodium concentration as a measure of tissue viability in nonhuman primate studies and in clinical studies. Radiology 1999;213:156–166.
15. Thulborn KR, Davis D, Adams H, Gindin T, Zhou J. Quantitative tissue sodium concentration mapping of the growth of focal cerebral tumors with sodium magnetic resonance imaging. Magn Reson Med 1999;41: 351–359.
16. Schepkin VD, Ross BD, Chenevert TL, et al. Sodium magnetic resonance imaging of chemotherapeutic response in a rat glioma. Magn Reson Med 2005;53:85–92.
17. Granot J. Sodium imaging of human body organs and extremities in vivo. Radiology 1988;167:547–550.
18. Steidle G, Graf H, Schick F. Sodium 2-D MRI of the human torso using a volume coil. Magn Reson Imaging 2004;22:171–180.